CHAPTER IV
RESULTS AND DISCUSSION

4.1 Precursor Synthesis

Silatrane and alumatrane were successfully synthesized via the Oxide One Pot Synthesis (OOPS) process. The FAB^+-MS results of crude products, silatrane and alumatrane, were shown in Tables 4.1 and 4.2, respectively.

Table 4.1 Proposed structure of silatrane using FAB^+-MS

m/e	Intensities	Proposed structure
174	100	$N[CH_2CH_2O]_3Si^+$
236	11.3	$H_2^+OCH_2CH_2OSi[OCH_2CH_2]_3N$
291	1	$N[CH_2CH_2O]_3OSiOCH_2CH_2N^+[CH_2CH_2OH]CH_2$
323	2.6	$H^+[HOCH_2CH_2]_2NCH_2CH_2OSi[OCH_2CH_2]_3N$
409	0.4	$N[CH_2CH_2O]_3H^+SiOCH_2CH_2OSi[OCH_2CH_2]_3N$

Table 4.2 Proposed structure of alumatrane using FAB^+-MS

m/e	Intensities	Proposed structure
192	100	$N[CH_2CHCH_3OH]_3H^+$ (TIS)
216	6.25	$N[CH_2CHCH_3O]_3H^+Al$ (monomer)
407	11.5	$H^+N[CH_2CHCH_3O]_3AlOH^+CHCH_3CH_2N[CH_2CHCH_3OH]_2$
431	19.25	$2N[CH_2CHCH_3O]_3H^+Al$ (dimer)
577	1.46	$[HOCHCH_3CH_2N[CH_2CHCH_3O]_2AlOCHCH_3CH_2]_2N^+CH_2$
646	0.38	$3N[CH2CHCH3O]3H+Al$ (trimer)

FT-IR spectra in Figure 4.1 show the characteristic peaks of the silatrane and alumatrane products, as follows. Silatrane: 3422 cm^{-1} (ν OH), 2986-2861 cm^{-1} (ν CH), 2697 cm^{-1} (ν N→Si), 1459-1445 cm^{-1} (δ CH), 1351 cm^{-1} (ν CN), 1082 cm^{-1} (ν Si-O-C), 1049 cm^{-1} (ν CO), 579 cm^{-1} (ν N→Si) and oxirane ring series peak at 1276, 939, 916 and 794 cm^{-1}. Alumatrane: 3404 cm^{-1} (ν OH), 2937-2881 cm^{-1} (ν CH), 1650 cm^{-1} (ν OH overtone), 1460 cm^{-1} (δ CH), 1089 cm^{-1} (ν Al-O-C) and 500-800 cm^{-1} (ν Al-O).
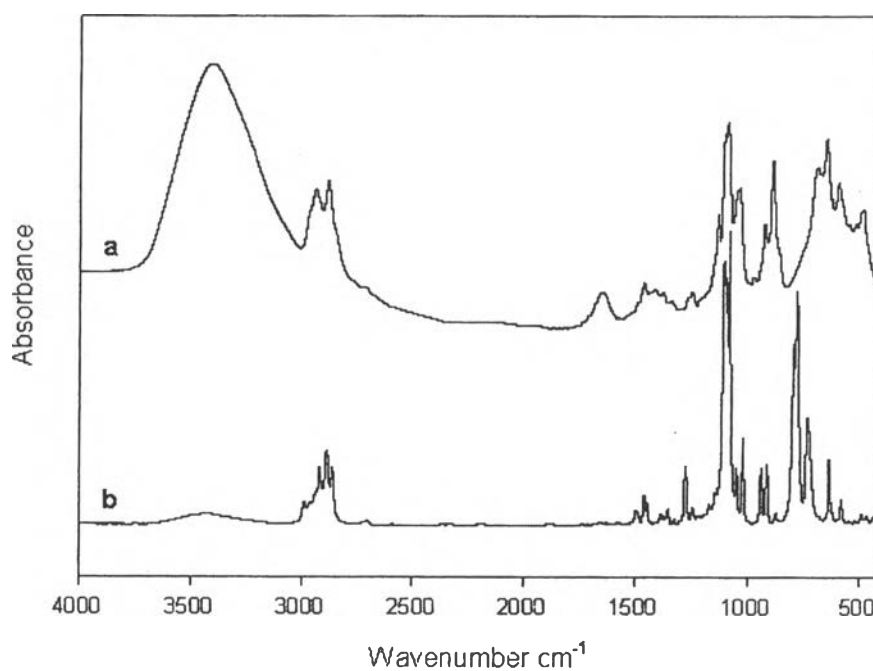
Figure 4.1 FT-IR results of a) alumatrane and b) silatrane.

TGA themograms of both silatrane and alumatrane were shown in Figure 4.2. Silatrane gives only one transition of weight loss at around 400°C, corresponding to the decomposition of organic ligand. The ceramic yield was around 18-22%. Alumatrane showed two major transitions at 140°C and 380°C referring to the organic ligand and carbon residue decompositions, respectively. The ceramic yield was around 30%.
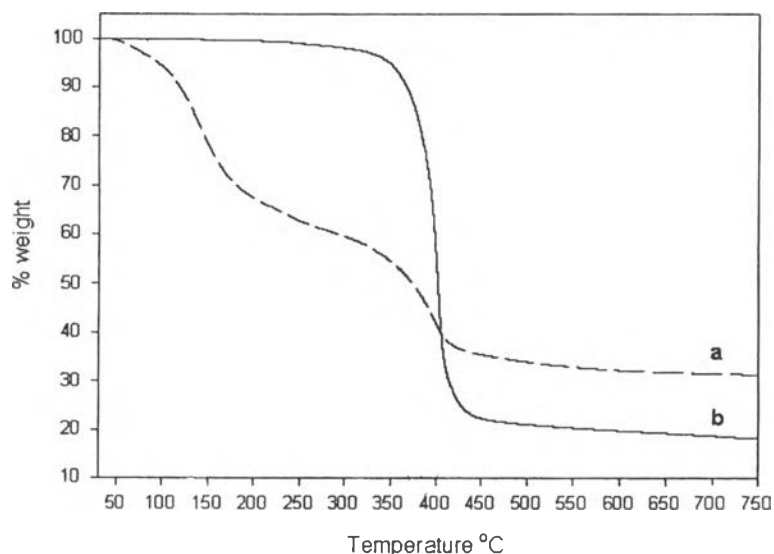
Figure 4.2 TGA results of a) alumatrane and b) silatrane.

4.2 Catalyst Preparation

In this work, tetrapropylammoniumbromide (TPABr) was used as the organic template for synthesizing silicalite-1 and ZSM-5 while FAU did not require the template for synthesis. The synthesis mixture concentration was fixed at the optimal mole ratio of $SiO_2:XAl_2O_3:0.1TPABr:0.4NaOH:114H_2O$, the aging and hydrothermal treatment time of 90 and 15 hr, respectively. The optimal mol ratio of synthesis mixture and condition for FAU synthesis was obtained from Sathupunya et al.'s work. The procedure requires a shorter time, 72 hr aging time and 5 hr hydrothermal treatment time with the concentration of $SiO_2:0.5Al_2O_3:2LiOH:410H_2O$. Microwave heating technique was employed in the hydrothermal treatment step due to a shorter heating time required.

The XRD results can confirm the structural type of the synthesized ZSM-5 zeolites when compared with the reference pattern of ZSM-5 in Figure 4.3. The significant peaks occur at the 2 theta range of 7-8 and 22-25 degree. The peak intensity depends on the degree of crystallinity related to the amount of aluminium loading.
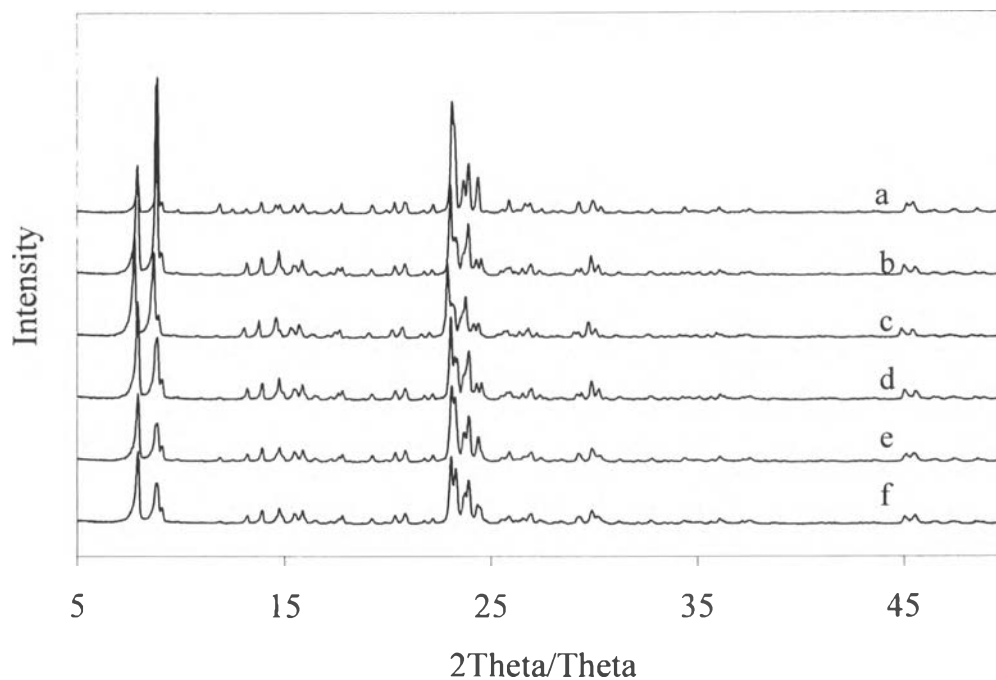
Figure 4.3 XRD results of H-ZSM-5 at different SiO_2/Al_2O_3 ratio a) reference, b) 250, c) 200, d) 150, e) 100 and f) 50.

The SEM results show the morphology of the ZSM-5 and FAU zeolites, see Figure 4.4. The average crystal sizes of both synthesized ZSM-5 and FAU zeolites at all Si/Al ratios were around 1-2 micron. There was no amorphous silica observed for the ZSM-5 crystals while the FAU crystals had some amorphous materials remaining in the structure. The shape of crystal was rounder as increasing amount of aluminium content for ZSM-5.
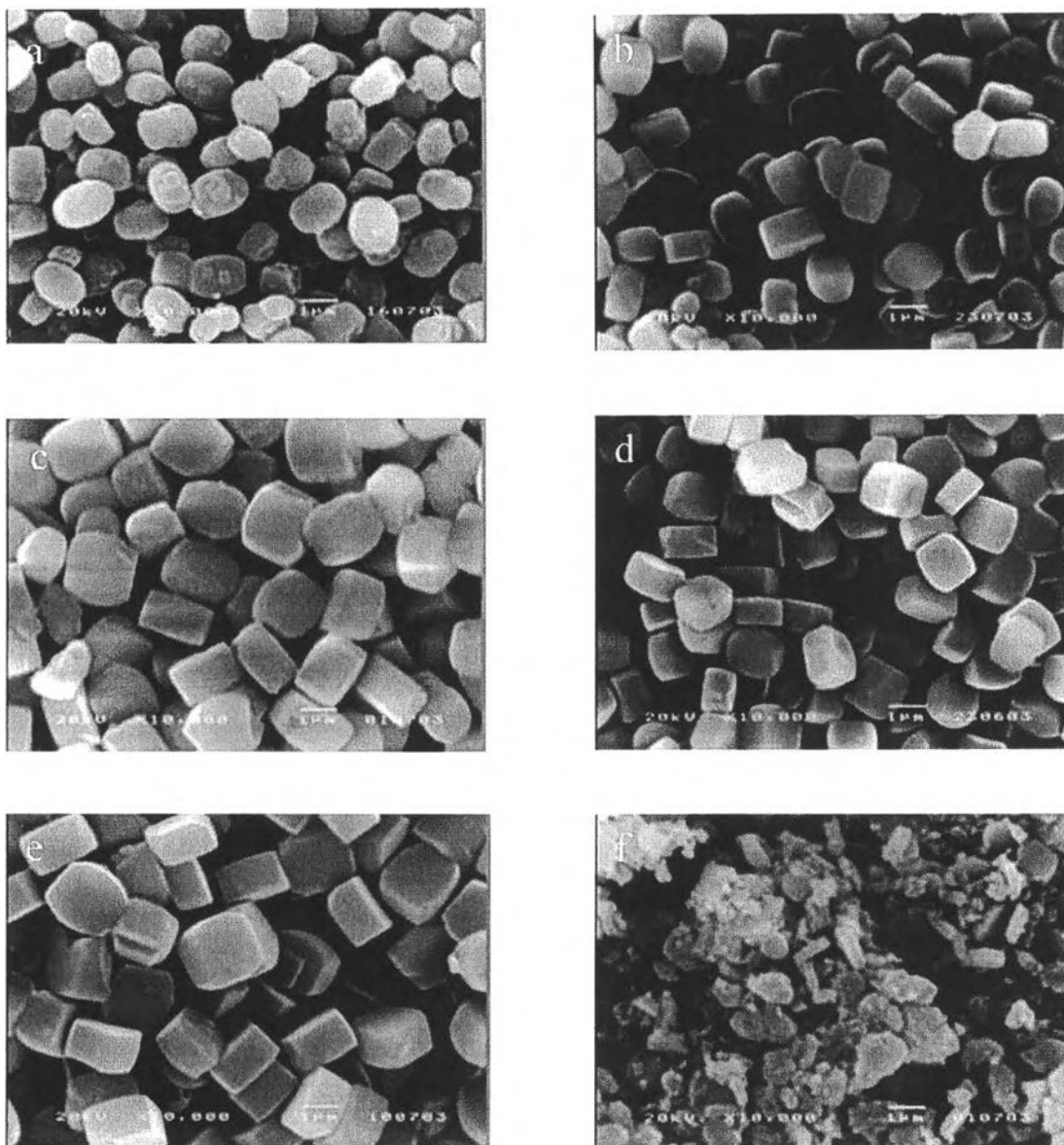
Figure 4.4 SEM results of synthetic zeolites at different SiO_2/Al_2O_3 ratio a) ZSM-5 50, b) ZSM-5 100, c) ZSM-5 150, d) ZSM-5 200, e) ZSM-5 250 and f) FAU.

The morphologies of the synthesized ZSM-5 were better than that of the commercial ZSM-5 in terms of crystallinity and homogeneity, as shown in Figure 4.5. The crystal shape of synthesized ZSM-5 was cubic while the commercial one was hexagonal crystal. The crystal size of commercial ZSM-5 was larger than that of the synthesized one.
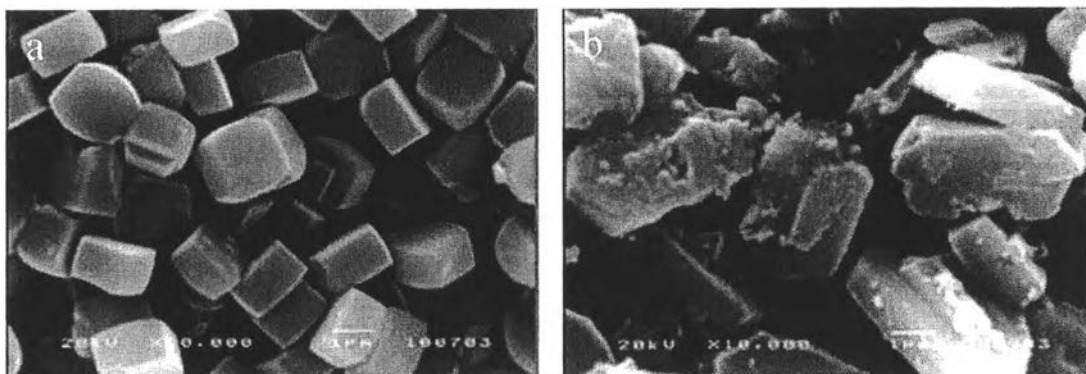
Figure 4.5 SEM results of a) synthesized ZSM-5 and b) commercial ZSM-5.

On the other hand, the morphologies of commercial 13X and Y zeolites at Si/Al ratio 2.34 and 3.43 were better than that of the synthesized FAU while the average crystal size was the same (Figure 4.6).
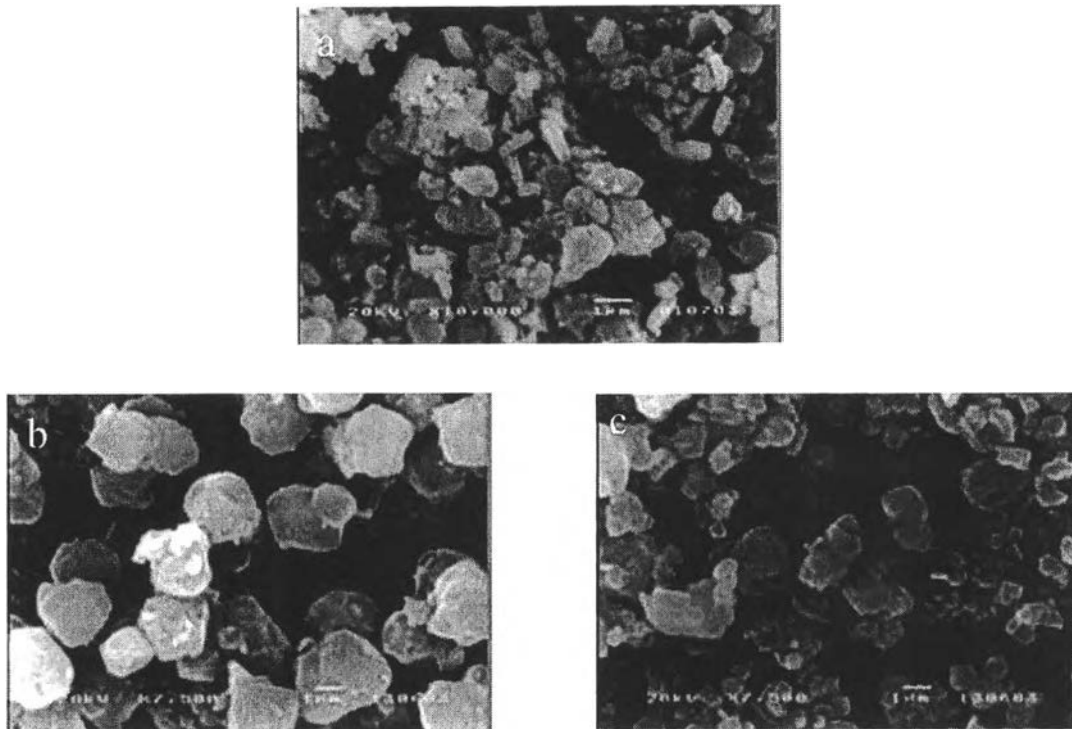
Figure 4.6. SEM results of a) Synthesized FAU, b) Commercial 13X and c) Commercial Y.

The comparison of the surface area and pore volume between synthesized and commercial ZSM-5 and FAU zeolites was listed in Table 4.3.

Table 4.3 Surface area and pore volume of zeolites

Zeolite	SiO_2/Al_2O_3 ratio	Surface area (m^2/g)	Pore volume (cm^3/g)
Com.H-ZSM-5	25	326	0.195
Syn.H-ZSM-5	50	445	0.279
Syn.H-ZSM-5	100	416	0.267
Syn.H-ZSM-5	150	453	0.279
Syn.H-ZSM-5	200	440	0.260
Syn.H-ZSM-5	250	450	0.266
Syn.H-FAU	1	603	0.314
Com.13X	2.34	724	0.424
Com.HY	3.43	689	0.343

In agreement with the SEM result, the total surface area of commercial H-ZSM-5 was lower than the synthesized H-ZSM-5. The pore volume also indicated lesser in void fraction in the channel of commercial H-ZSM-5. It can be concluded that the physical properties of the synthesized ZSM-5 via silatrane and alumatrane are better than the commercial ZSM-5.

The amount of elements in the synthesized zeolites was investigated using XRF technique. The result is shown in Table 4.4. The SiO_2/Al_2O_3 ratio in each sample from XRF result showed slight deviation from the calculated value. It indicated that the amount of Si and/or aluminium loaded in the synthesis step was not completely reacted.

Table 4.4 Elemental analysis for SiO_2/Al_2O_3 ratio of zeolites by XRF

Zeolite	Claculated SiO_2/Al_2O_3	Actual SiO_2/Al_2O_3
Syn.H-ZSM-5	50	43.20
Syn.H-ZSM-5	100	96.75
Syn.H-ZSM-5	150	111.36
Syn.H-ZSM-5	200	173.83
Syn.H-ZSM-5	250	256.07
Com.H-ZSM-5	-	24.98
Syn.FAU	1	1.16

Acidity measurement was obtained using TPD technique. Figure 4.7 shows pyridine TPD spectra of H-ZSM-5 zeolites at all SiO_2/Al_2O_3 ratios (50-250). Under this condition, the maximum desorption temperature for each sample was around 300°C. The amount of chemisorption pyridine corresponded to the peak area of each sample. It was found that acidity increases as the SiO_2/Al_2O_3 ratio decreases.
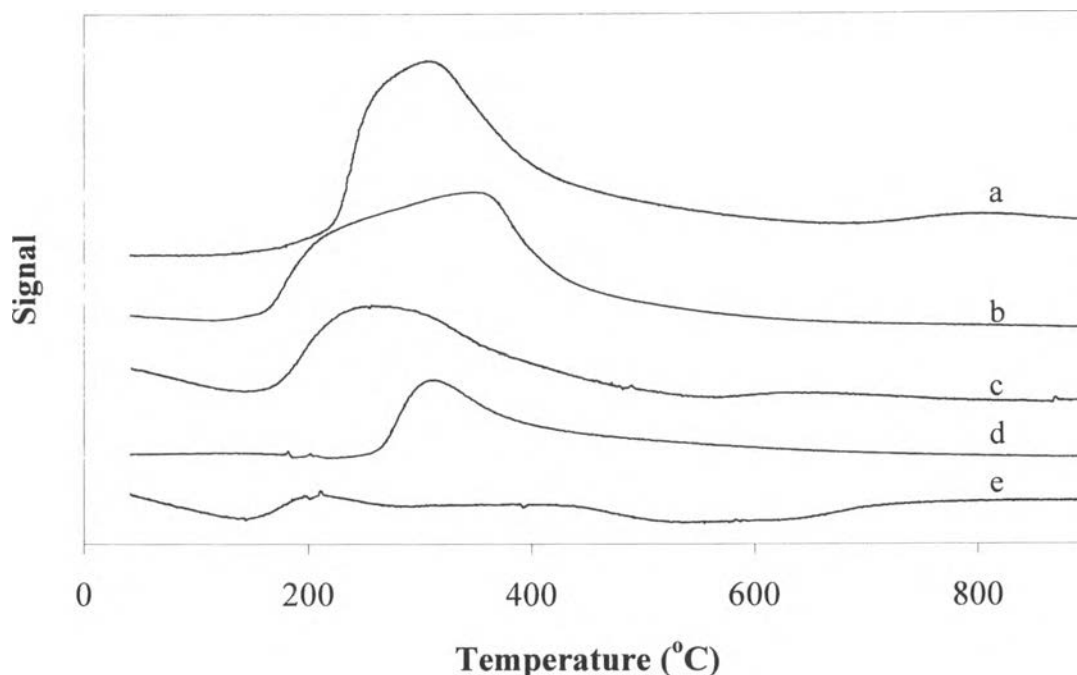
23

Figure 4.7 TPD spectra of H-ZSM-5 zeolites at all SiO_2/Al_2O_3 ratios a) 50, b) 100, c) 150, d) 200 and e) 250.

4.3 Catalyst Modifications

4.3.1 Seeding Technique: Effect of Dilution

The crystal growth of silicalite-1 and ZSM-5 was studied by seeding technique with these crystals. It is known that the non-selective acid sites at the external surface of zeolites play the major role in degrading the shape selectivity. The aim of this study was thus to eliminate these external acid sites. It had been proposed that a layer might be grown over the seed crystal in a two-step synthesis. ZSM-5 core crystal continues to grow, forming an outer shell of silicalite. The deposition of silica layer on the ZSM-5 has been under investigation.

Seeding was performed on TPA-ZSM-5 crystals using various concentration of seeding solutions: $Si:H_2O$ = 1:114 (solution 1.A), $Si:H_2O$ = 1:1000 (solution 2.A), $Si:H_2O$ = 5000 (solution 3.A), $Si:H_2O$ = 200 (solution 4.A) and $Si:H_2O$ = 250 (solution 5.A). SEM images of TPA-ZSM-5 seed crystals and seeding products are shown in Figure 4.8. The average crystal sizes of ZSM-5 seed were around 2 micron (Figure 4.8a). The preferential growth in the concentrate synthesis

solution 1.A, the same molar ratio as ZSM-5 seed preparation, reveals the earliest stage of the seed crystal growth (Figure 4.8b). The crystal sizes of seed product were around 2.5-3 micron. It can be indicated that new layer of silicalite-1 overgrown on the seed crystals. However, there were some secondary nucleation occurring on the product surface at this concentrate solution ($Si:H_2O$ = 1:114), especially on B direction. Therefore, the product crystals were spotted with new crystallites growing in an ordered manner.

In contrast to the previous observations, the silicalite seed crystals at more dilute solutions, 2.A and 3.A ($SiO_2:H_2O$ = 1:1000 and 1:5000), at the fixed pH are shown in Figure 4.8c and 4.8d, respectively. The discrete products with smaller crystal sizes were obtained. The amount of seed products remaining from two-step crystallization at these 2 concentrations were only 10 percent when compared with the theoretical calculation at 100 percent growth yield. It can be concluded that the use of high amount of the strongly alkaline media caused the dissolution of the seed crystals back into the solution.
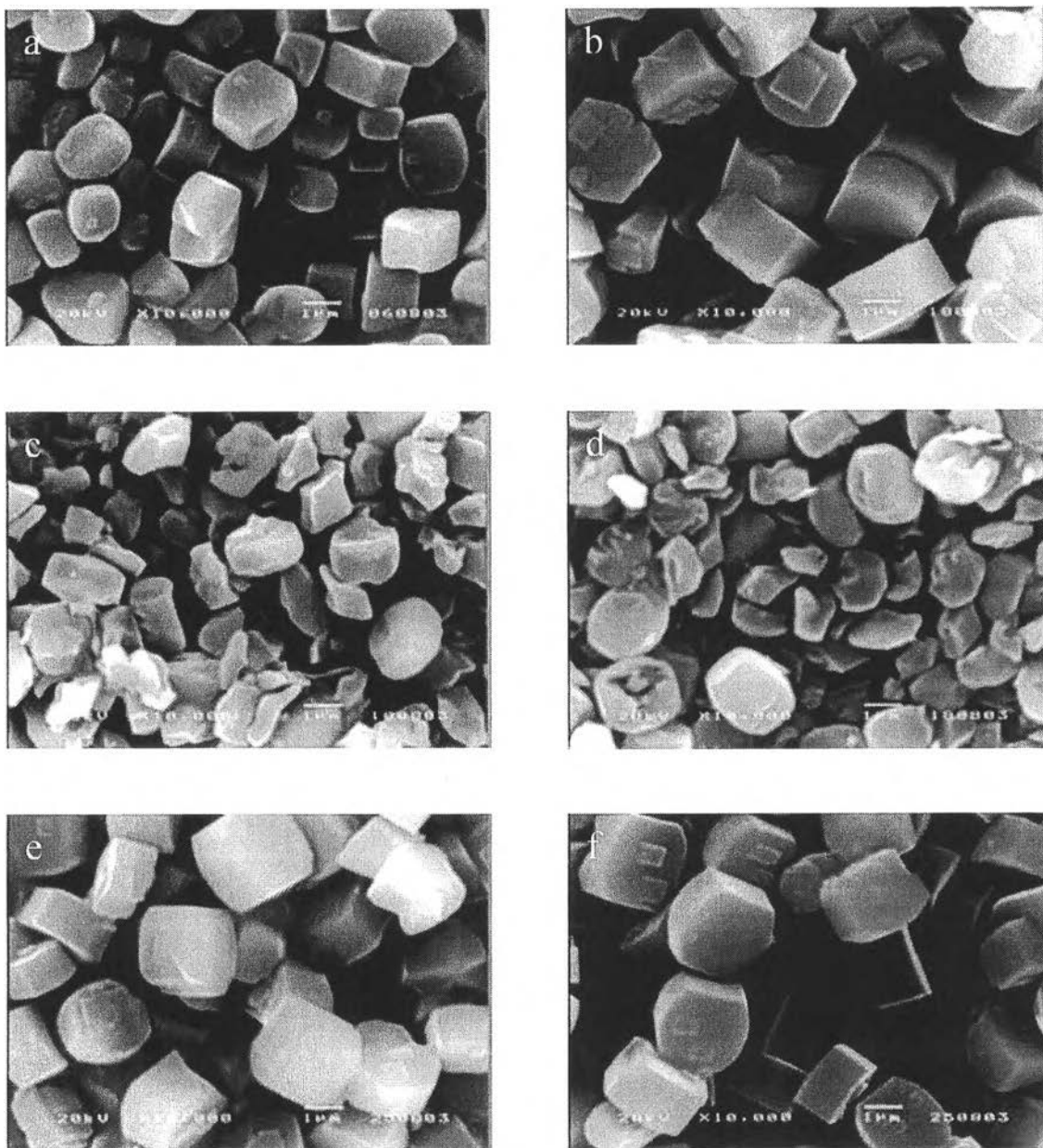
Figure 4.8 SEM results of ZSM-5 seed and seeding product a) TPA-ZSM-5 seed, b) seed 1.A, c) seed 2.A, d) seed 3.A, e) seed 4.A and f) seed 5.A.

XRD patterns in Figure 4.9 show the diffractograms of TPA-silicalite-1, TPA-ZSM-5 seed and seed product 1.A. The result can be confirmed that there was no change in the crystal structure of the seed product when compared with ZSM-5 seed. The peak intensity of seed product 1.A at 8 degree 2θ was between the ZSM-5 seed and silicalite-1.
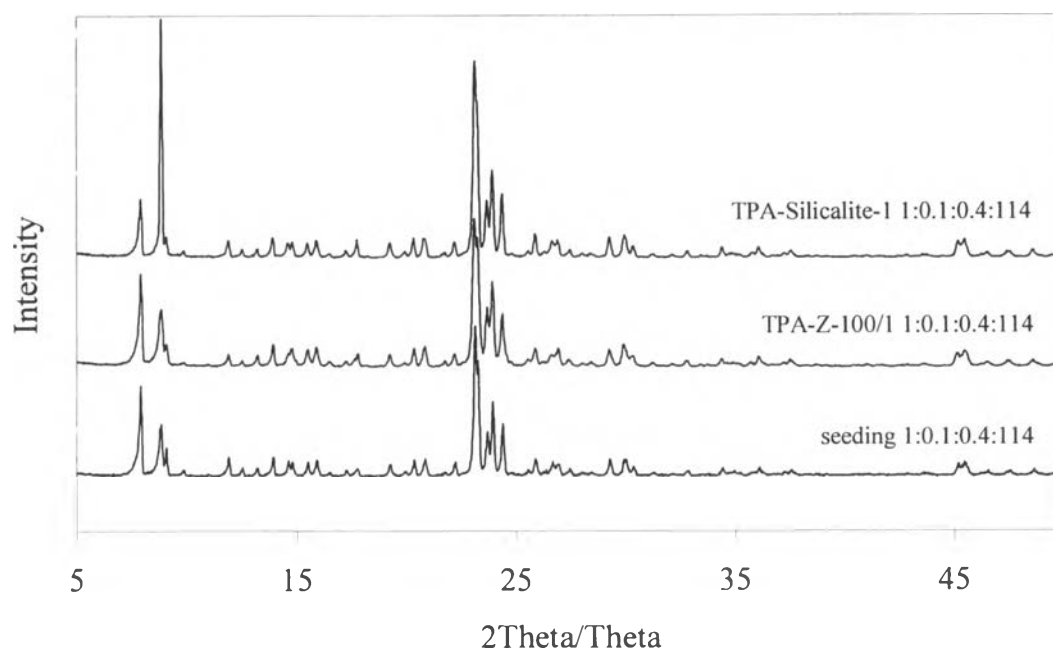
Figure 4.9 XRD patterns of TPA-silicalite-1, TPA-ZSM-5 seed and seed product 1.A.

For more observation in the change of XRD patterns, the characteristic peaks in the range of 22.5-25 degree 2θ were investigated and are shown in Figure 4.10. Firstly, the plane (501) reflection was dominant whereas the (051) reflection became more significant by increasing the amount of aluminium loading. Since the unit cell of silicalite-1 was smaller than that of ZSM-5 due to the difference in size of silicon and aluminium molecular ion, (501) reflection was shifted to the higher degree at lower aluminium content in the unit cell. However, this distortion effect did not occur with other reflection peaks. The peak intensity of the seed product 1.A was higher than TPA-ZSM-5 seed. This indicates that the seed product had more preferential orientation of the silicalite-1 shell coating on the surface of ZSM-5 seed. The (133) reflection peak of the seed product became more significant when compared with the same reflection peaks of high aluminium ZSM-5 at SiO_2/Al_2O_3 ratio of 50 and ZSM-5 seed. This is another evidence to confirm that the silicalite-1 was coated on the seed surface.

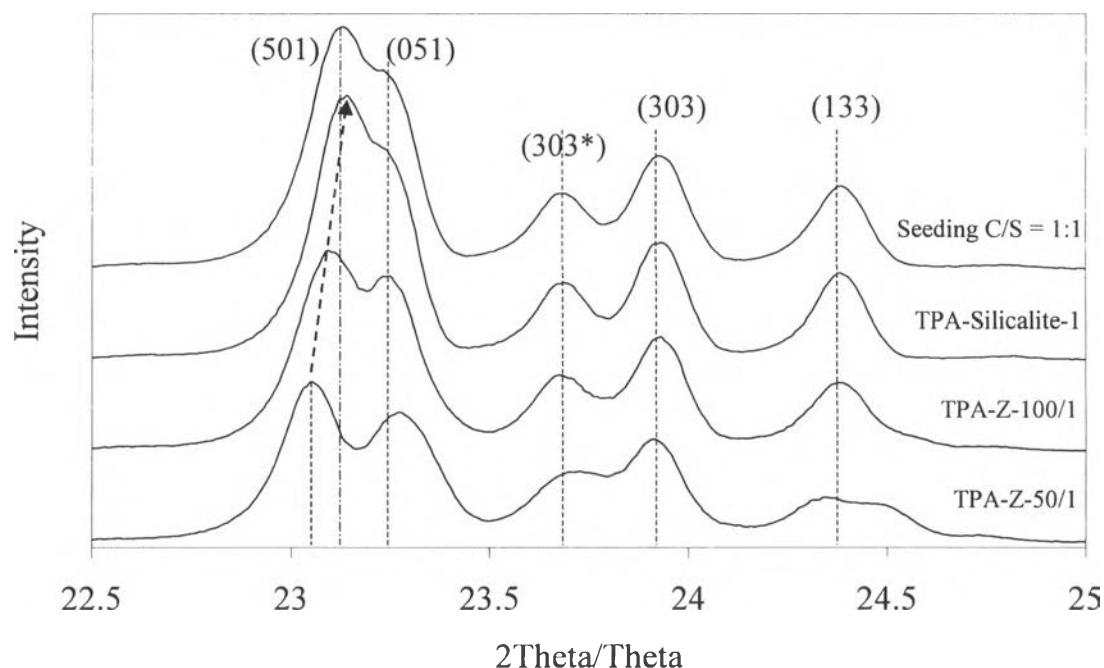**Figure 4.10** XRD patterns of seed product 1.A, TPA-silicalite-1, TPA-ZSM-5 seed and ZSM-5 SiO_2/Al_2O_3 ratio 50.

However, there was some secondary nucleation on the seed product at concentrated system 1.A. This was probably due to the competition between the growth rate of existing crystals and nucleation rate of new crystal on the surface. Which process predominated, depended on their relative rates and whether a stage of supersaturation. To reduce the nucleation rate, more dilute solution with milder alkaline environment was studied. Similar to the concentrated solution, the larger size of seed crystals in more dilute synthesis mixtures 4.A and 5.A at H_2O/SiO_2 molar ratio of 200 (Figure 4.8e) and 250 (Figure 4.8f) were still obtained when compared with TPA-ZSM-5 seed. It indicates that the crystal growth still occurs even in more dilute system. The crystal surface was clearer due to the lower nucleation rate on the surface. The XRD patterns of the seed products at three dilution systems are shown in Figure 4.11. There was no difference in the position and intensity of all dilution ratios.
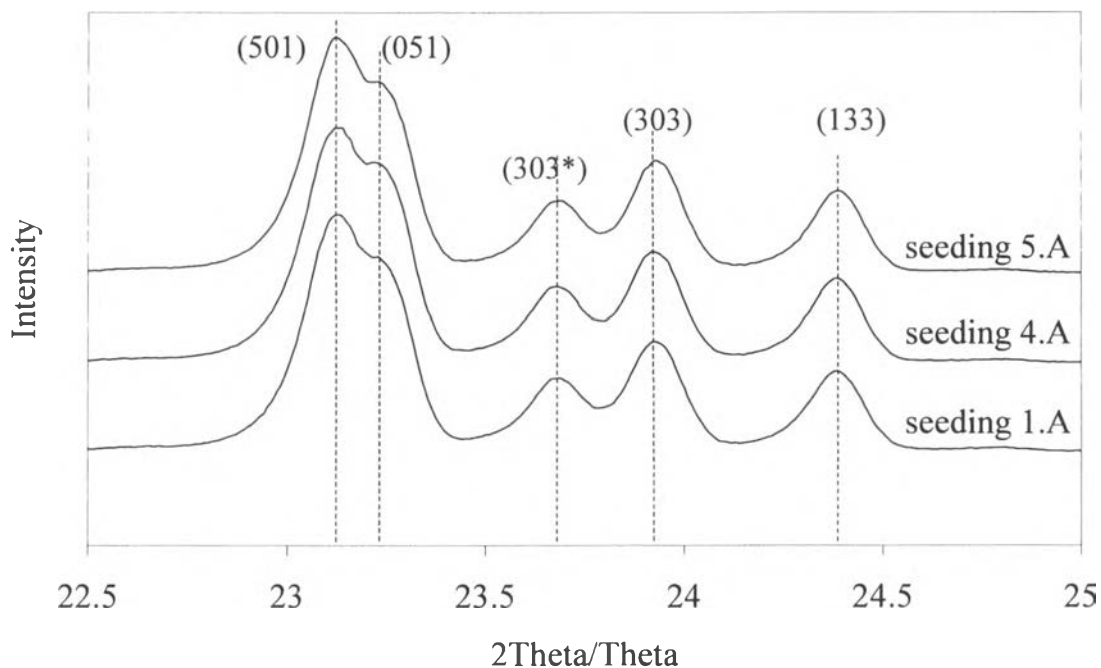
Figure 4.11 XRD patterns of the seed products at three dilution systems.

To determine whether the silicalite-1 totally coated on the surface, TPD of large base molecule of 4-methyl quinoline (4-MQ) was conducted, as shown in Figure 4.12. The TPD spectra of modified sample showed an extraordinary decrease in the amount of external acid site, as compared with ZSM-5 seed. The result was confirmed by comparing with pure silicalite-1, indicating that the external surface acidity was totally covered by coating.
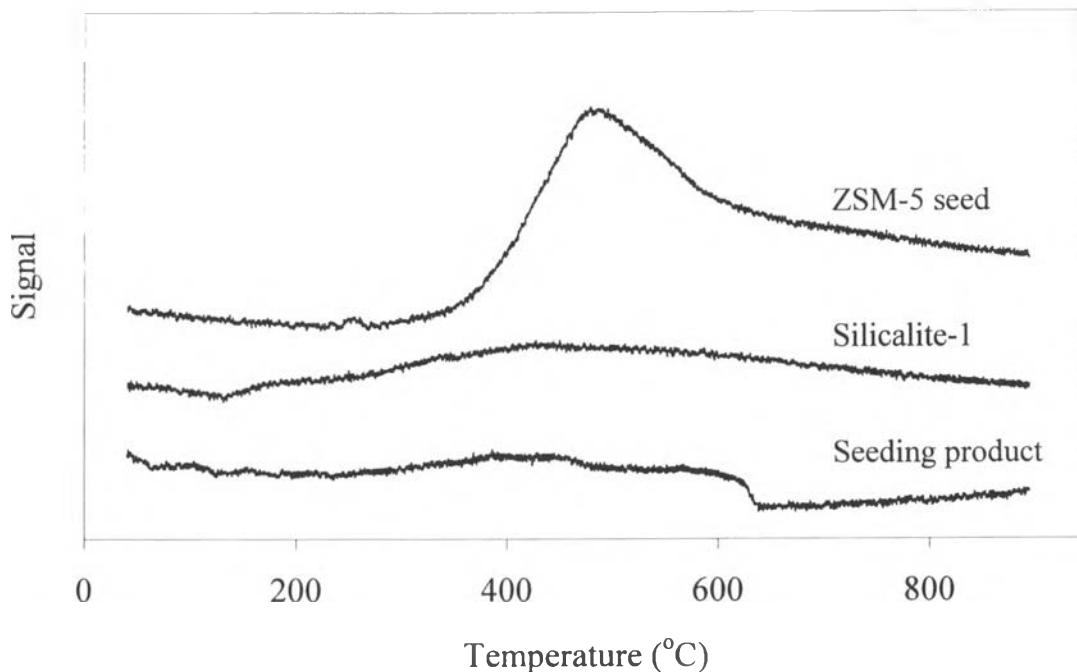
(

Figure 4.12 4-MQ TPD spectra of ZSM-5 seed, silicalite-1 and seed product.

4.3.2 Chemical Vapor Deposition (CVD)

From the previous work, there were several parameters affecting to the silica deposition efficiency of CVD method. In this work, the H-ZSM-5 with three different aluminium concentrations were studied to investigate the effect of external surface acidity on the amount of silica deposited and also the change of catalytic properties.

4.3.2.1 TEOS Breakthrough Curve

The deposition of TEOS was observed at space velocity of 5 h^{-1}, 200°C by using 6.38% by volume of TEOS in methanol solvent as a feed. The breakthrough curve for a CVD of ZSM-5 zeolite at the SiO_2/Al_2O_3 ratio of 250 is shown in Figure 4.13.
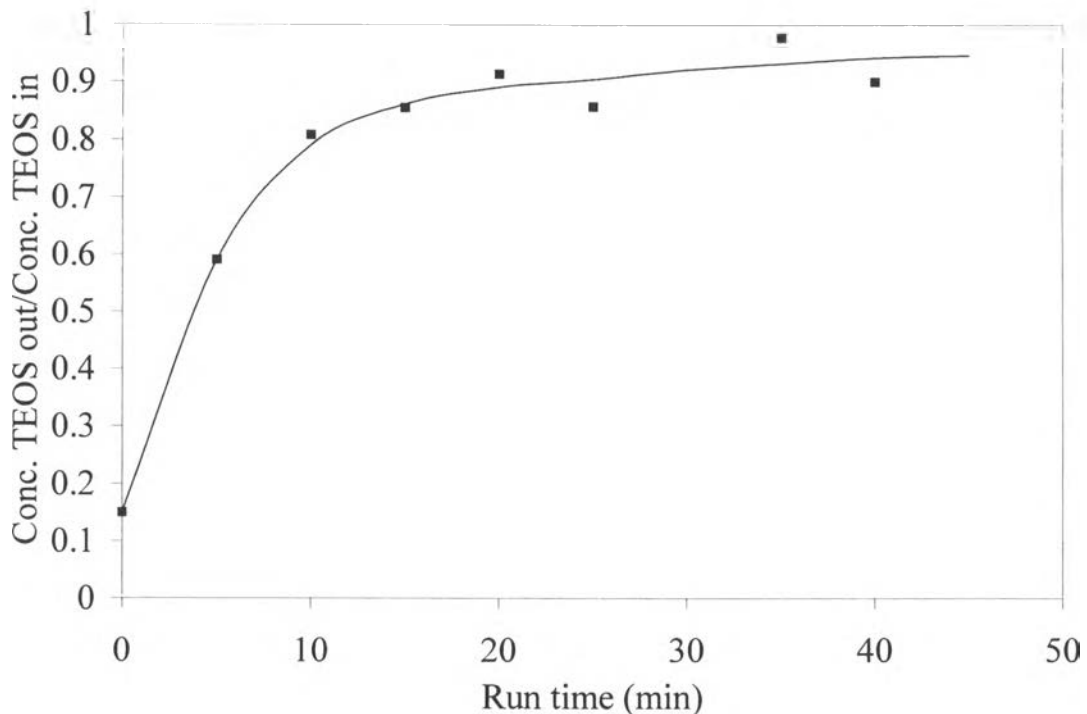
Figure 4.13 TEOS breakthrough curve for a CVD of ZSM-5 zeolite.

At the first time, almost 85 percent of TEOS deposited on the zeolite surface. The concentration of TEOS at the outlet reached constant after 30 min of stream released. It indicates that the external surface of zeolite was totally covered with TEOS. Therefore, the effective time for the first CVD cycle of TEOS was around 30 min.

4.3.2.2 Effect of ZSM-5 Acidity on CVD of TEOS

The results from CVD treatment of ZSM-5 zeolites at three different SiO_2/Al_2O_3 ratios after 30 min run time are shown in Table 4.5. It was found that the amount of deposited silica was related to the acidity of ZSM-5 zeolites. The highest amount of silica deposited, 0.96% wt of catalyst, was observed from the highest Al- containing H-ZSM-5 at the SiO_2/Al_2O_3 ratio of 50. This indicates that the number of acid sites on zeolite promoted the deposition of TEOS. The amount of silica deposited increased when the acid density increased. The increase of temperature during deposition showed highly exothermic heat of

adsorption of TEOS on the external acid sites of ZSM-5. That means, the deposition of TEOS was the chemisorption type, just forming only monolayer coverage at the first step. The maximum temperature increased depended on the acid strength of each ZSM-5 sample.

Table 4.5 Amount of silica deposited on H-ZSM-5 from CVD of TEOS

Zeolite	SiO_2/Al_2O_3 ratio	Al content (atom/unit cell)	Amount of SiO_2 deposited (%wt)
Syn.H-ZSM-5	50	3.84	0.96
Syn.H-ZSM-5	150	1.28	0.41
Syn.H-ZSM-5	250	0.77	0.28

The SEM and BET results in Figure 4.14 and Table 4.6, respectively, do not show any difference in the morphology and surface area between modified H-ZSM-5 and fresh H-ZSM-5 catalysts at all SiO_2/Al_2O_3 ratios. It indicates that one cycle surface modification using CVD technique did not change the morphology and surface area of zeolites.
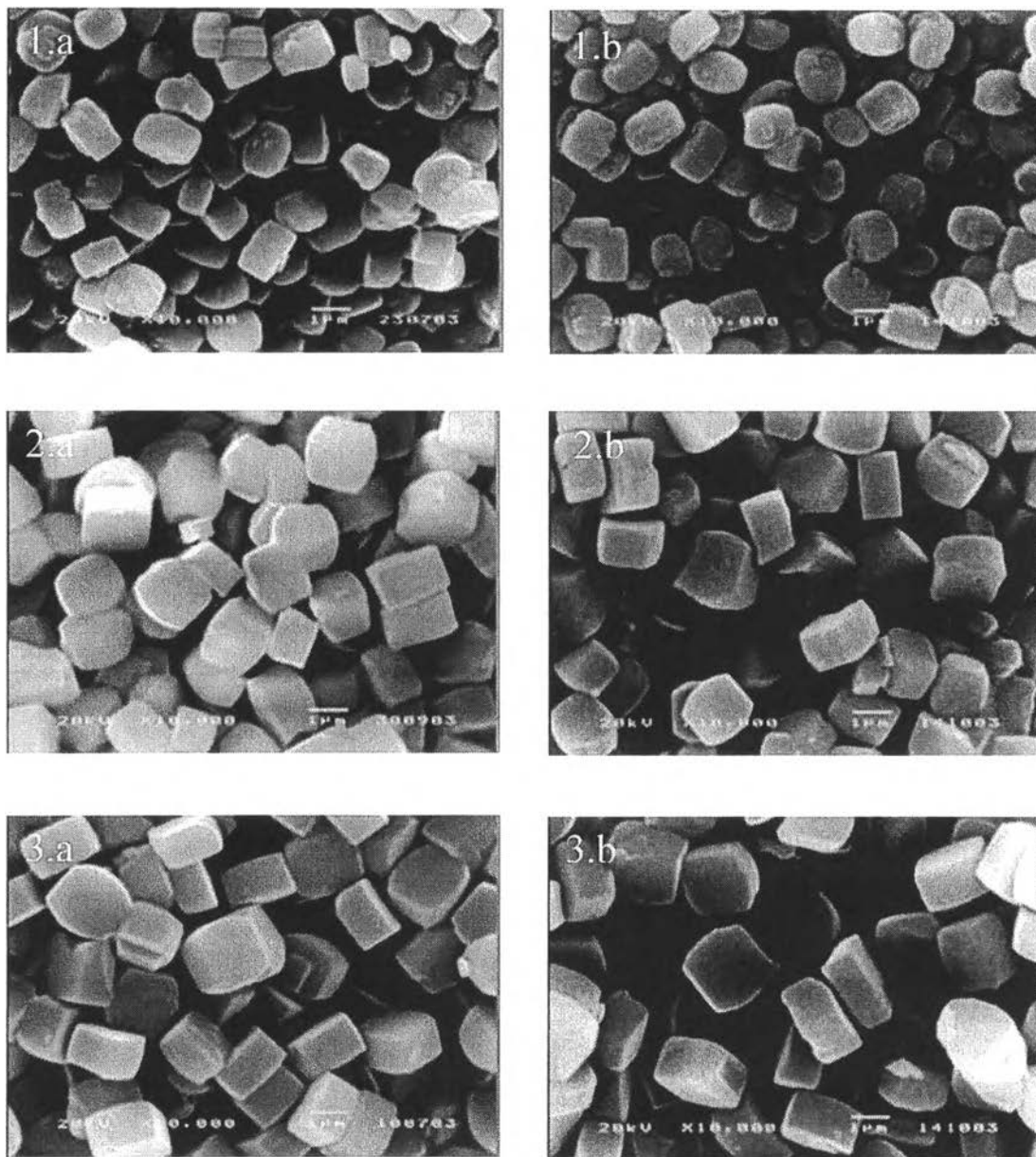
Figure 4.14 SEM results of fresh and modified ZSM-5 by CVD method at different SiO_2/Al_2O_3 ratio 1.a) fresh 50, 1.b) modified 50, 2.a) fresh 150, 2.b) modified 150, 3.a) fresh 250 and 3.b) modified 250.

Table 4.6 Surface area and pore volume of modified and unmodified ZSM-5

Zeolite	SiO_2/Al_2O_3	Surface area (m^2/g)	Pore volume (cm^3/g)
H-ZSM-5	50	410	0.252
Modified H-ZSM-5	50	400	0.243
H-ZSM-5	150	453	0.279
Modified H-ZSM-5	150	452	0.279
H-ZSM-5	250	450	0.266
Modified H-ZSM-5	250	446	0.260

Similarly, with CVD technique, temperature programmed desorption (TPD) of 4-MQ was also used to probe the acidity of ZSM-5 before and after modification. Samples were pretreated with nitrogen gas at 250°C for 1hr to remove moisture. Helium was used as a carrier gas during desorption stage. The TPD signals of modified and unmodified ZSM-5 at the SiO_2/Al_2O_3 ratio of 50 are shown in figure 4.15. The relative amount of 4-MQ adsorption/desorption from CVD modified ZSM-5 at the SiO_2/Al_2O_3 ratio of 50 was approximately 60.86% of the unmodified sample. Maximum desorption temperature for modified and unmodified ZSM-5 was around 480° and 510°C, respectively. The relative signals from CVD modified ZSM-5 at the SiO_2/Al_2O_3 ratio of 150 and 250 represented higher percentage areas at 78.67% and 75.32%, respectively (Figure 4.16 and Figure 4.17). In agreement with the amount of silica deposited, low aluminium containing ZSM-5 has lower activity to adsorb silicon alkoxide than high aluminium containing ZSM-5. This probably is because wider distance between two Si-O-Al bridge acid sites obstructs the silica layer formation above the surface.
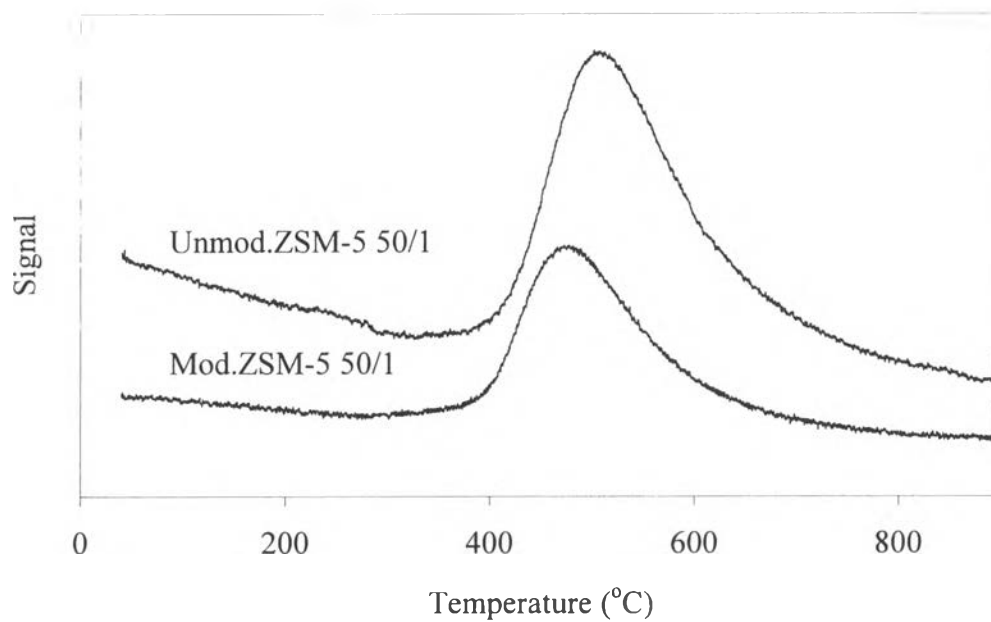
Figure 4.15 4-MQ TPD spectra of CVD modified and unmodified ZSM-5 with SiO$_2$/Al$_2$O$_3$ ratio 50.

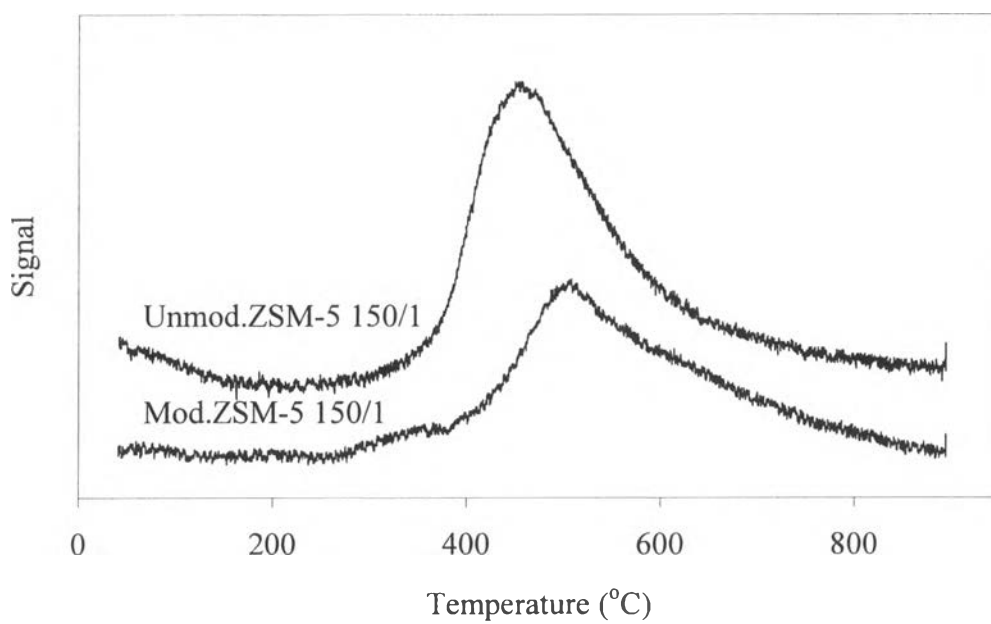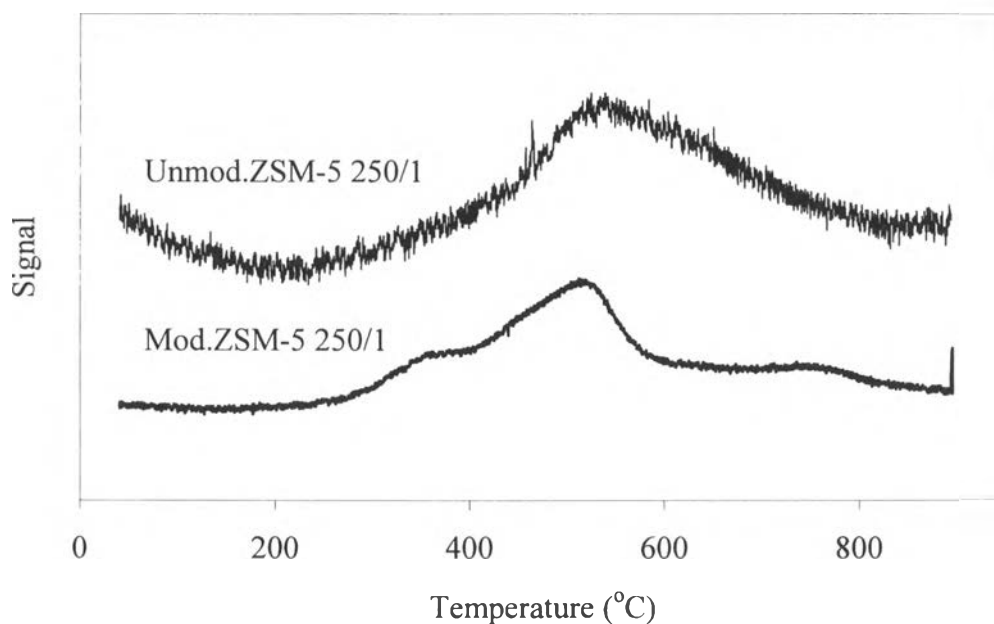**Figure 4.16** 4-MQ TPD spectra of CVD modified and unmodified ZSM-5 with SiO$_2$/Al$_2$O$_3$ ratio 150.

Figure 4.17 4-MQ TPD spectra of CVD modified and unmodified ZSM-5 with SiO$_2$/Al$_2$O$_3$ ratio 250.

4.4 Toluene Disproportionation Activity of ZSM-5

The reaction testing had been done under atmospheric pressure and temperature in the range of 400°-500°C. Toluene were fed with WHSV 100 hr^{-1} and mixed with nitrogen carrier gas at the flow rate of 8 ml/min before passing through the reactor. The catalyst bed contained 0.4 g of catalyst in each run. The effluent products from the reaction were analyzed by gas chromatography.

4.4.1 Deactivation Time

The breakthrough curve of toluene conversion at 400°C is shown in Figure 4.18. The catalyst was totally deactivated around 40 min running time. However, this also depends on the acid strength of the zeolite. The zeolite pores were blocked leading to a decrease in the conversion.
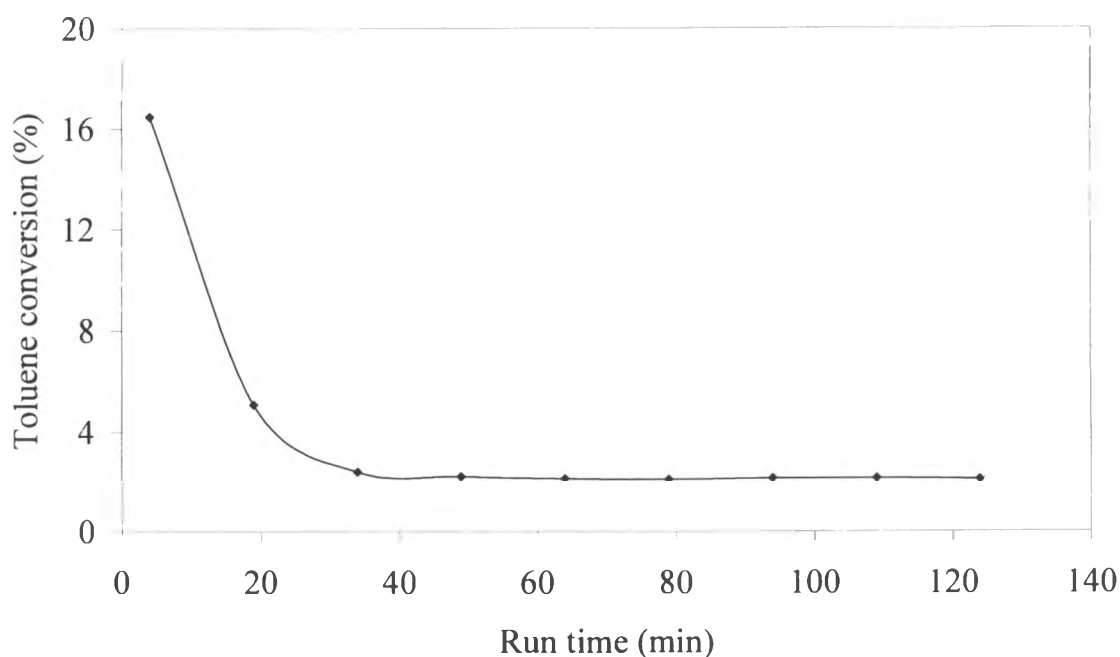
I 916 18768

Figure 4.18 ZSM-5 deactivation curve at 400°C.

4.4.2 Comparison between Synthesized and Commercial ZSM-5

The results from toluene disproportionation reaction at 500°C 130 min time-on-stream for commercial and synthesized ZSM-5 zeolites are shown in Table 4.7.

Table 4.7 Toluene disproportionation reaction results of commercial and synthesized ZSM-5 zeolites

Zeolite	SiO_2/Al_2O_3	Conversion (%)	Para-selectivity (%)	B/X ratio
Com.ZSM-5	25	29.08	55.33	1.32
Syn. ZSM-5	25	36.33	30.76	1.28

At the same SiO_2/Al_2O_3 ratio, the first stage conversion for synthesized ZSM-5 was higher than commercial ZSM-5. On the other hands, para-selectivity of commercial ZSM-5 was 20% higher than synthesized ZSM-5. This result corresponded to the characterization results. A higher surface area promoted a

higher conversion while the crystal size had strong effect on the product selectivity. The larger crystal size zeolite contains the lesser fraction of external surface area when compared to the total surface area. Therefore, the non-selective acid sites on the external surface of zeolite were decreased when the crystal size increased. However, the selectivity into p-xylene for both 2 catalysts is higher than thermodynamic equilibrium value at 24:52:24. The benzene /xylene ratio for both 2 catalysts was higher than the thermodynamic equilibrium value of 1. It is possible that the xylene products were converted to the other products at strong acid environment or dealkylation of toluene to yield more benzene and methane. Similar result for toluene conversion was obtained by Bhaskar and Do (1990), the activity of both HZSM-5 was initially high and then rapidly decreased as time progress, see Figure 4.19a. Figure 4.19b shows an increase in para-selectivity corresponded with time on steam. This is probably because the coke formation narrowed the pore of zeolite and also passivated the acid sites on external surface. The difference in the crystal size of zeolite catalysts played an important role in the step of increasing para-selectivity. The para-xylene yield using commercial ZSM-5 was higher than synthesized ZSM-5 at the first stage of conversion, as shown in figure 4.19c. However, p-xylene yield for both 2 catalysts eventually became equal as time on stream increased. The plot between benzene/xylene v.s. time, which corresponds with the selectivity toward disproportionation, is shown in Figure 4.19d. The B/X ratio using synthesized ZSM-5 was slightly higher than that using commercial ZSM-5 and reached steady after 30 min running time. This might be because of the difference in acid strength that promoted different side reaction (toluene dealkylation and xylene disproportionation) rate, producing more benzene and other products.
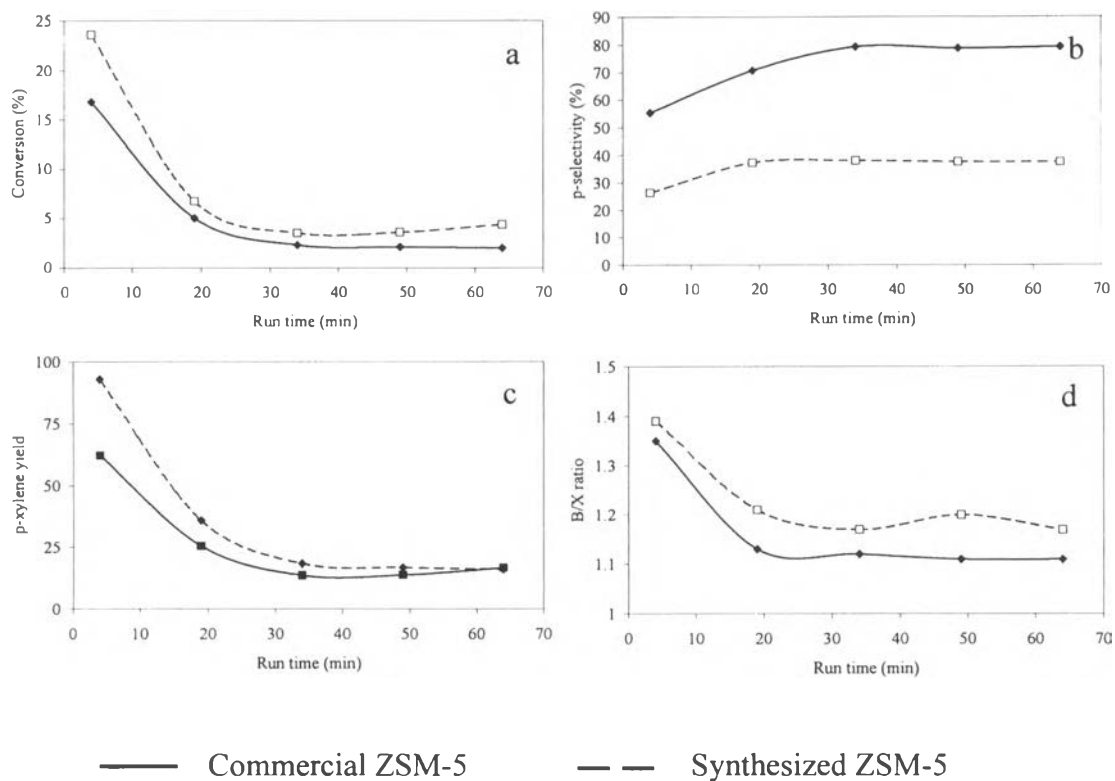
Figure 4.19 Comparison between synthesized and commercial ZSM-5 (SiO_2/Al_2O_3 ratio = 25): a) Toluene conversion, b) p-selectivity, c) p-xylene yield and d) B/X ratio.

The study on the effect of temperature in toluene disproportionation reaction was performed at 2 different temperatures (400°C and 500°C). The results from the reaction are summarized in Table 4.8.

Table 4.8 Effect of temperature on toluene disproportionation reaction

Zeolite	Temperature ($^{\circ}$C)	SiO$_2$/Al$_2$O$_3$	Conversion (%)	Para-sel (%)	B/X ratio
Com.ZSM-5	400	25	16.46	55.33	1.32
Com.ZSM-5	500	25	29.08	55.84	1.35
Syn.ZSM-5	400	50	5.17	28.82	1.28
Syn.ZSM-5	500	50	19.60	33.37	1.35

After increasing the temperature, toluene conversion was increased for both commercial and synthesized ZSM-5 zeolites. However, the para-selectivity still remained nearly the same value. This indicates that the increase in temperature did not affect to the product selectivity. The catalysts were deactivated faster at 500°C because the coking rate increased rapidly at high temperature.

4.4.3 Effect of SiO$_2$/Al$_2$O$_3$ Ratio

The investigation on the effect of SiO$_2$/Al$_2$O$_3$ ratio in toluene disproportionation reaction at 500°C for synthesized ZSM-5 with SiO$_2$/Al$_2$O$_3$ ratio in the range of 50-250 is shown in Figure 4.20a. Toluene conversion highly increased at low SiO$_2$/Al$_2$O$_3$ ratio. There was slightly difference in conversion for ZSM-5 at SiO$_2$/Al$_2$O$_3$ over than 100. The para-selectivity did not significantly change for all SiO$_2$/Al$_2$O$_3$ ratios, as shown in Figure 4.20b.
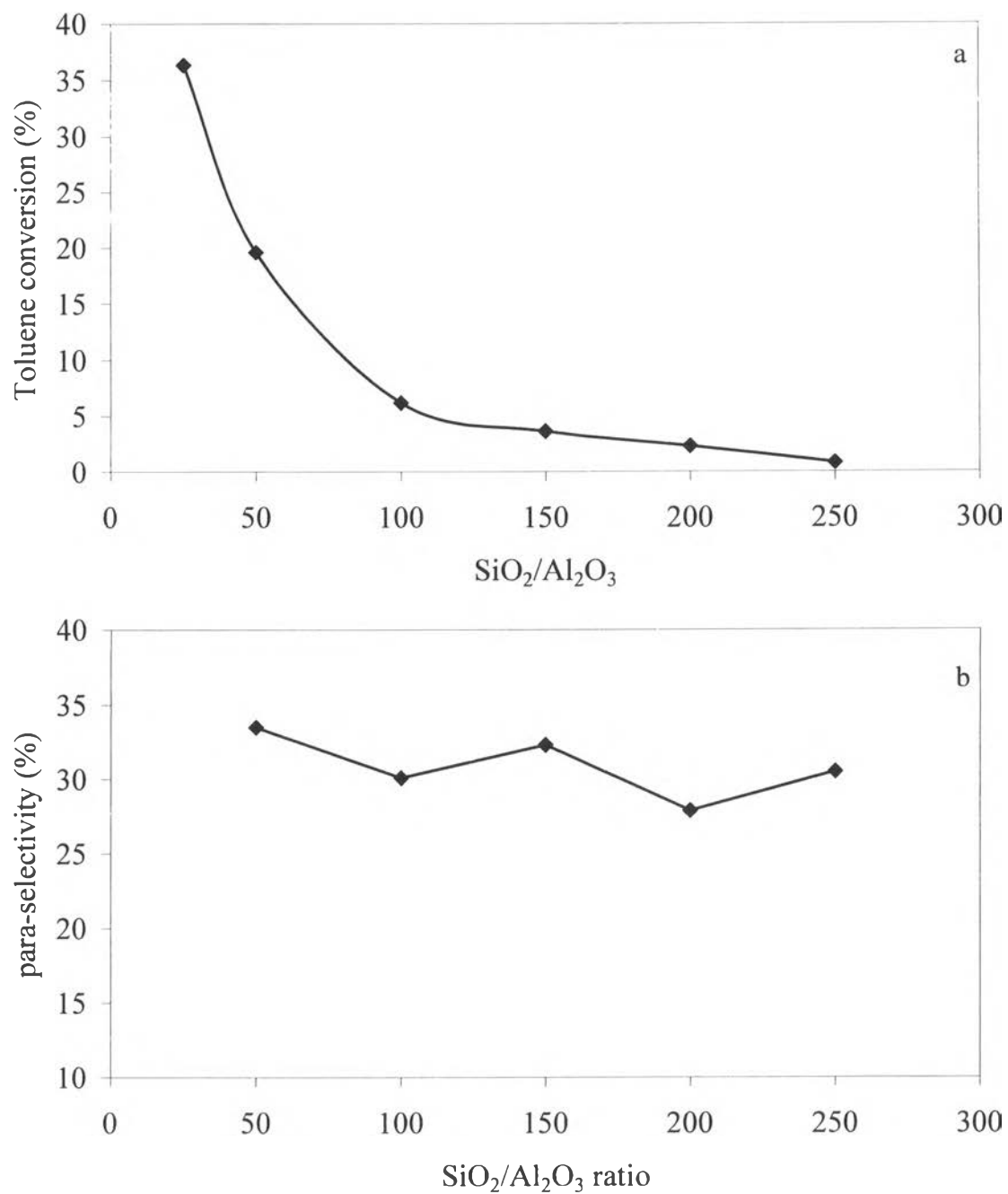
Figure 4.20 Effect of SiO$_2$/Al$_2$O$_3$ ratio a) Toluene conversion and b) Selectivity of p-xylene.

4.4.4 Catalytic Activity of CVD Modified ZSM-5

The normalized first stage conversion from three different SiO_2/Al_2O_3 ratios of CVD modified ZSM-5 at 50, 150 and 250 were observed (Figure 4.21a). The conversion of ZSM-5 at the 50 SiO_2/Al_2O_3 ratio was 20% dropped down after modification while the other ratios gave no significant change. It is probably due to excessive silica partially blocked on pore opening and caused diffusional constraint. The enhancement of para-selectivity after surface modification is shown in Figure 4.21b. Different result was observed by Manstein *et al.* (2002), which the para-selectivity could be increased up to 90 percent with only one modification cycle for ZSM-5 at the 50 SiO_2/Al_2O_3 ratio. This result confirmed that non-selective acid sites on the external surface had strong effect on the product selectivity. The para-xylene yield was doubled for CVD modified ZSM-5 at all SiO_2/Al_2O_3 ratios, as shown in Figure 4.21c. Monitoring the deactivation of modified catalyst on toluene disproportionation indicated results in contrast with Uguina *et al.* (1992). Figure 4.22 shows the deactivation of CVD modified ZSM-5 catalyst compared with unmodified ZSM-5 at the SiO_2/Al_2O_3 ratio of 50. The catalyst was still deactivated after inertized the external surface acidity. This indicates that the coke formation could occur even in the zeolite pore.
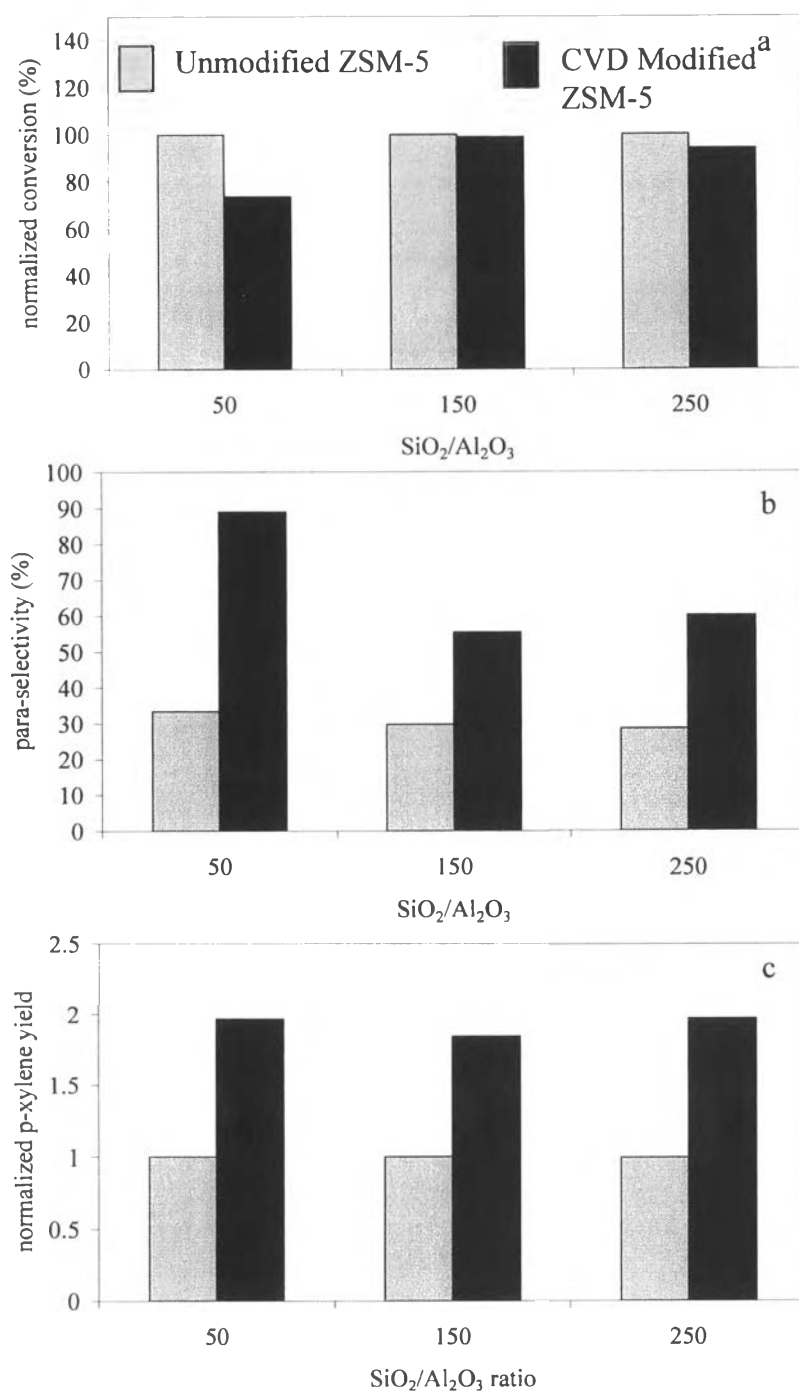
Figure 4.21 Disproportionation activity of CVD modified ZSM-5: a) Toluene conversion, b) p-selectivity and c) p-xylene yield.
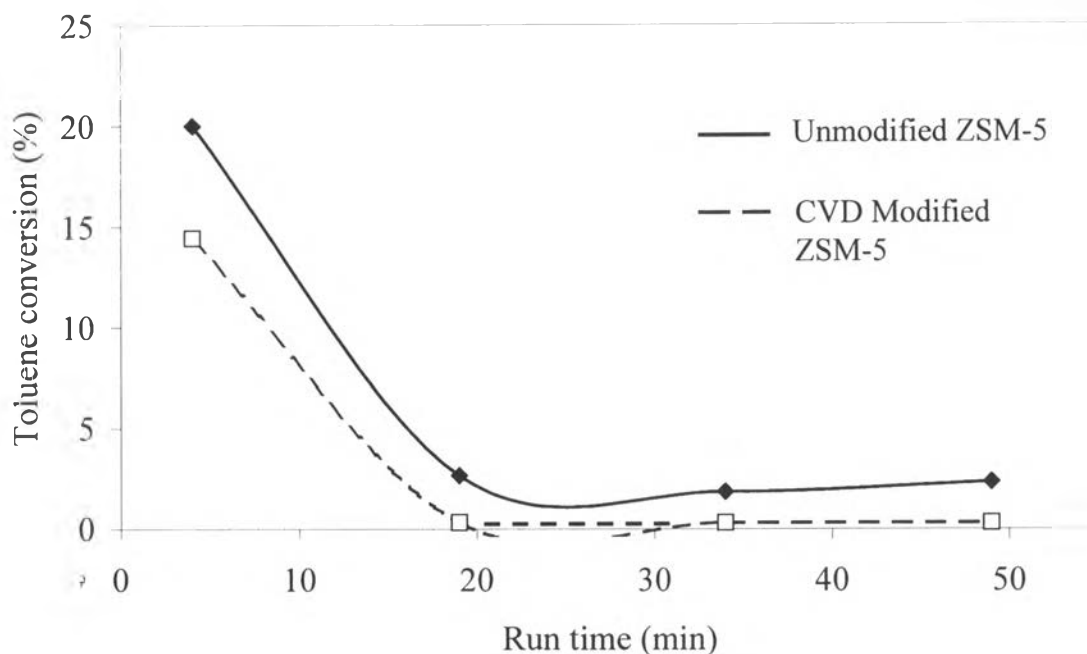
Figure 4.22 Deactivation of CVD modified ZSM-5.

4.4.5 Catalytic Activity of Silicalite Shell Modified ZSM-5

The ZSM-5 zeolite with the SiO_2/Al_2O_3 ratio of 50 was used as seed for the modification. The modified product had core/shell weight ratio of 1. This value was obtained from the secondary synthesis mixture yielding 2 grams of product per gram of ZSM-5 seed added. The amount of modified sample used for the reaction testing was double of the unmodified sample. This is because the silicalite shell decreased the mass of ZSM-5 seed per gram of sample. The reaction results of modified sample compared with unmodified catalyst are summarized in Table 4.9. Unlike CVD modified ZSM-5, the first stage conversion of the seed product hardly decreased when compared with unmodified sample. This indicates that modification using this technique gives no effect on the structure and pore of ZSM-5. The para selectivity was enhanced to around 75 percent. However, the difference in the crystal size between seeding and CVD modified catalysts might have some effect in the selectivity enhancement. The para selectivity of CVD modified ZSM-5 was higher than silicalite shell modified sample. This might be because the surface of CVD modified zeolite consisted of inert silica while that of

silicalite-1 still presented some of low acidic silanol groups. The comparison in para-xylene yield between unmodified and those 2 methods of surface modification are shown in Figure 4.23. It seems that the silicalite shell modification gave higher para-xylene yield than the CVD technique.

Table 4.9 Disproportionation activity of modified ZSM-5 catalysts compared with unmodified catalyst

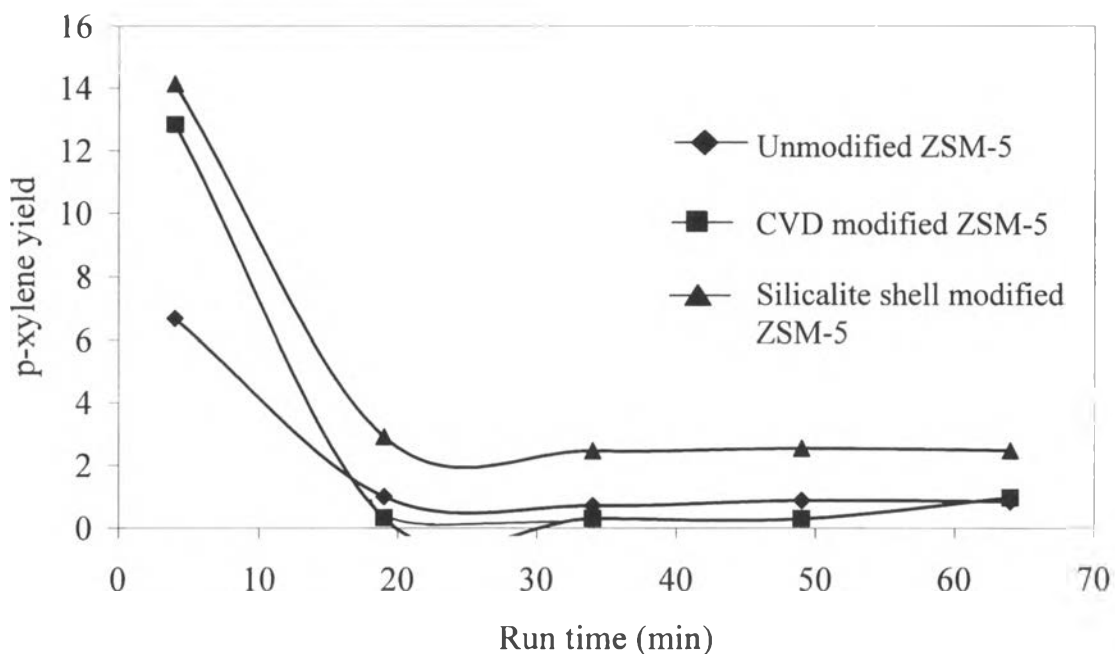| Catalyst	Conversion (%)	Para-selectivity (%)
Unmodifed ZSM-5	20.0	33.7
CVD modified ZSM-5	14.4	89.0
Silicalite shell mod. ZSM-5	19.2	73.6

Figure 4.23 P-xylene yields between modified and unmodified ZSM-5.

4.5 Toluene Disproportionation Activity of FAU

Even though faujasite zeolite has higher aluminium content in unit cell than ZSM-5 zeolite, the result from FAU zeolite was not impressive, as can be seen in Table 4.10.

Table 4.10 Reaction results from FAU zeolites

Zeolite	SiO_2/Al_2O_3	Conversion (%)	P-selectivity (%)
Commercial 13X	2.34	1.92	28.5
Commercial Y	3.43	0.35	29.8
Synthesized FAU	1	0.13	28.0

It might be due to the difference of Si-O-Al angles in its framework causing the difference in acid strength.